JOC The Journal of Organic Chemistry

pubs.acs.org/joc Article

The Nature of Azo-Substituted Carbocations: N–N π-Electron Stabilization versus Nitrogen Nonbonding Electron Stabilization

Xavier Creary*

Cite This: https://dx.doi.org/10.1021/acs.joc.1c00140 Read Online

ACCESS | Metrics & More | Article Recommendations | Supporting Information

ABSTRACT: Computational and experimental studies reveal two different modes of cation stabilization by the phenylazo group. The first mode involves a relatively weak conjugative interaction with the azo π-bond, while the second mode involves an interaction with the nitrogen nonbonding electrons. The 4-phenylazo group is slightly rate-retarding in the solvolysis of cumyl chloride and benzyl mesylate derivatives but rate-enhancing in the solvolysis of α-CF_3 benzylic analogs. The phenylazo group can become a potent electron-donating group in cations such as $[Me_2C{-}N{=}N{-}Ph]^+$. Nonbonding electron stabilization can be strong enough to offset the very powerful γ-silyl stabilization. In aromatic cyclopropenium and tropylium cations, the demand for stabilization is quite low, and the mode of phenylazo stabilization reverts back to the less-effective π-stabilization. The solvolysis of *cis*-4-phenylazo benzyl mesylate is faster than that of *trans*-4-phenylazo benzyl mesylate. Products formed suggest a stepwise ionization, cation isomerization, and nucleophile capture mechanism. Computational studies indicate a vanishingly small barrier for the isomerization of the *cis*-cation intermediate to the *trans*-cation.

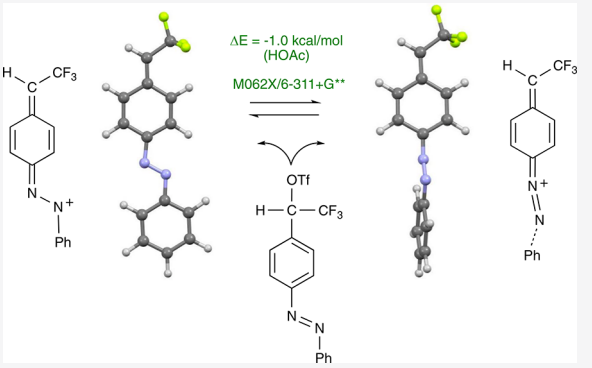

INTRODUCTION

Azo compounds of general structure **1** contain one of the most important functional groups in chemistry (Figure 1).[1] Azo dyes

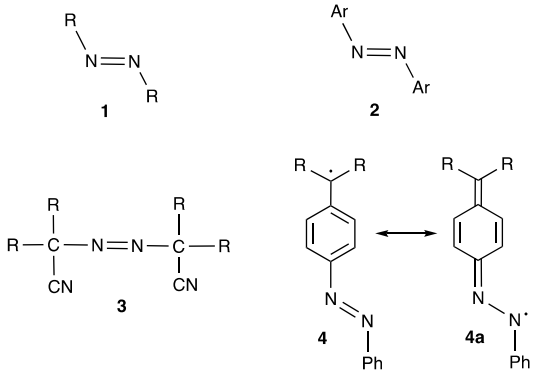

Figure 1. Compounds containing the azo functional group.

2, despite their potential toxicity, are used in a myriad of industries due to their range of colors.[2] They also have numerous biomedical applications, which have been recently reviewed.[3] Azo compounds such as **3** can serve as a source of radicals and are often used as initiators in polymerization.[4] Other azo compounds have found use in actinometry and in other photochemical applications.[5] Our previous interest in the azo group was due to its radical-stabilizing properties.[6] Due to a very large π-stabilizing conjugative interaction, the phenylazo group in **4** has been termed a "super radical stabilizer".[6]

In view of the π-type stabilizing conjugative interaction in radical **4**, analogous interactions in carbocations are also of interest. Cations of general structure **5**, i.e, azo-substituted carbocations, were therefore of interest. Such carbocations fall under the general category of cations substituted with formally electron-withdrawing groups, i.e., cations of general structure **6**. Such carbocations, as illustrated by **7**–**9** (Figure 2), have been

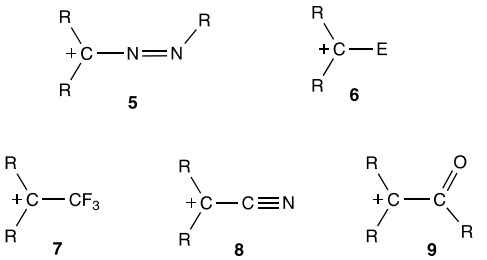

Figure 2. Carbocations with formally electron-withdrawing groups.

Received: January 18, 2021

extensively studied in the past[7,8] and can often be generated solvolitically. In many instances, the solvolytic rates of generation for cations **8**[9] and **9**[10] far exceed what would be expected on the basis of the formal electron-withdrawing properties of the cyano and carbonyl groups.

It has been suggested that certain electron-withdrawing groups can also exert a cation-stabilizing resonance effect, as shown by forms **10b**,[11] **11b**, and **11c**[12] in Figure 3. Resonance stabilization by the cyano[9] and carbonyl[10] groups has also been suggested, but the importance of carbonyl resonance stabilization has been questioned.[13]

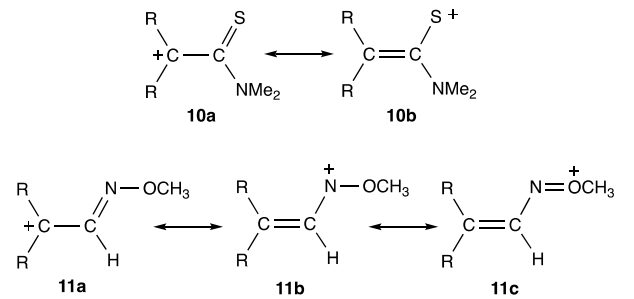

Figure 3. Resonance stabilization of carbocations with electron-withdrawing groups.

The phenylazo group is formally electron-withdrawing, as indicated by the Hammett σ_p value of +0.34.[14,15] Cations of type **5** have been proposed as intermediates in the reaction of α-chloroazo compounds **11** with Lewis acids (Scheme 1).[16] These

Scheme 1. Generation of α-Azo Cations

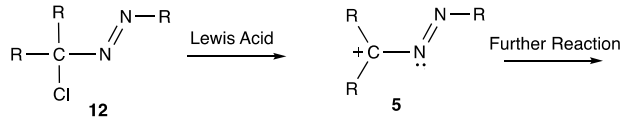

cations can undergo many fascinating inter- and intramolecular reactions. The following additional questions were also of interest. How easily are these cations generated under solvolytic conditions? How do they compare in terms of stability with other cations of general type **6**? What are the stabilization mechanisms for these cations? Are they stabilized by the N−N π-bond or the nitrogen nonbonding electrons? Reported here are experimental and computational studies on cations **5** that address these questions.

RESULTS AND DISCUSSION

Computational Studies on Cumyl Cations. The 4-phenylazocumyl cation **14** has previously been generated solvolytically to determine the Hammett−Brown σ^+ value.[15] Thus, the azo-substituted chloride **13** reacts 5.2× more slowly than cumyl chloride in 80% aqueous acetone (Scheme 2). This corresponds to a σ^+ value of +0.17 and suggests that the phenylazo group *destabilizes* the transition state, leading to the cation **14**. The structure of cation **14** has now been calculated[17] at the M062X/6-311+G** level. This structure **14a** (Figure 4) shows the N−N π-bond in conjugation with both aromatic rings. However, a careful examination of **14a** shows that the N−N−phenyl plane is rotated slightly (4.6°) out of planarity with the cumyl cation ring. This calculated structure is in agreement with the suggestion[15] that the nonbonding nitrogen electrons are not

Scheme 2. Solvolysis of 4-Azocumyl Chloride 13

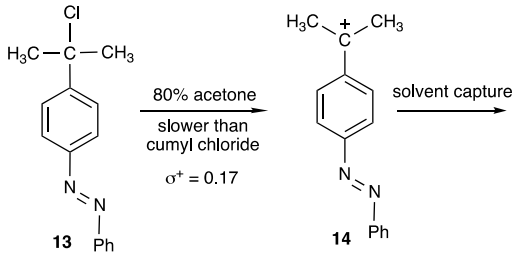

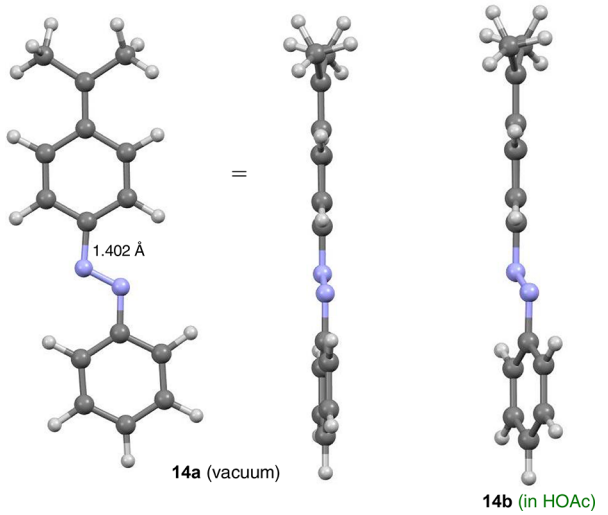

Figure 4. M062X/6-311+G**-calculated structure of the substituted cumyl cation **14**.

involved in the stabilization of **14a**. The structure of cation **14** has also been calculated in acetic acid, a commonly used solvent in solvolysis reactions, using the polarizable continuum model (PCM)[18] available in Gaussian 16. The resultant structure **14b** (in acetic acid) is slightly different from that of cation **14a** calculated in the gas phase. The rotation of the phenylazo group out of planarity increases to 19.2° in cation **14b** (where acetic acid is the solvent).

The isodesmic reaction shown in Scheme 3 has been used to evaluate the stabilizing or destabilizing effect of the phenylazo group on **14** relative to the unsubstituted cumyl cation **17**. This calculation places the *stabilization* of **14a** at 4.6 kcal/mol in the gas phase despite the fact that cation **14** forms less readily than the cumyl cation **17** under solvolytic conditions. When acetic acid is employed as the solvent in the calculation, cation **14b** is actually 1.1 kcal/mol *less stable* than the cumyl cation **17**. This is more in line with the experimental rate data observed in Scheme 2. Much of this reversal of cation stabilities from a vacuum to the acetic acid solvent is due to the greater solvent stabilization of the cumyl cation **17** relative to the solvent stabilization of the larger phenylazo-substituted cation **14**.

Benzylic Cation Studies. Attention was next focused on the substituted benzyl cation, where the demand for cation stabilization in this primary system should be greater than that in the tertiary cation **14**. This cation has now been generated under solvolytic conditions from the mesylate **20** in trifluoroethanol, CD_3CO_2D, and formic acid, where simple substitution products were observed. The rate of reaction (Table 1) was compared to that of unsubstituted benzyl mesylate **19**. The effect of the phenylazo group (Figure 5) is a minimal rate-

https://dx.doi.org/10.1021/acs.joc.1c00140
J. Org. Chem. XXXX, XXX, XXX−XXX

Scheme 3. Isodesmic Reaction of Phenylazocumyl Cation 14 with Cumene

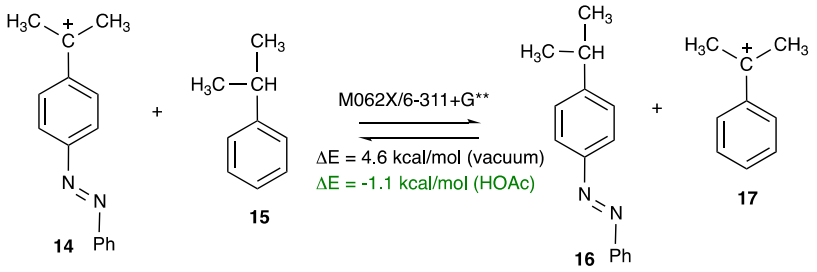

Table 1. Solvolysis Rates of Various Substrates

substrate	T (°C)	solvent	k (s^{-1})
19	21.5	CD_3CO_2D	2.98×10^{-6}
19	23.0	CF_3CH_2OH	2.14×10^{-4}
19	21.5	HCO_2H	2.66×10^{-3}
20	21.5	CD_3CO_2D	1.32×10^{-6}[a]
20	23.0	CF_3CH_2OH	1.57×10^{-4}
20	21.5	HCO_2H	1.03×10^{-3}
26	21.5	CD_3CO_2D	4.84×10^{-5}
48	21.5	CD_3CO_2D	3.43×10^{-5}
48	21.5	CF_3CH_2OH	8.63×10^{-3}
49	21.5	CD_3CO_2D	4.43×10^{-6}
49	21.5	CF_3CH_2OH	7.13×10^{-4}
53	21.5	CD_3CO_2D	7.39×10^{-3}
58	21.5	CD_3CO_2D	1.48×10^{-4}
59	21.5	CD_3CO_2D	2.07×10^{-7}[b]
60	21.5	CD_3CO_2D	1.66×10^{-7}[c]

[a]The value of 1.19×10^{-6} s^{-1} was used when comparing the rate of **20** to **26**. See the Supporting Information. [b]Extrapolated value from k at 60.0 °C = 3.45×10^{-5} s^{-1} and k at 40.0 °C = 2.83×10^{-6} s^{-1}. [c]Extrapolated value from k at 60.0 °C = 2.92×10^{-5} s^{-1} and k at 40.0 °C = 2.33×10^{-6} s^{-1}.

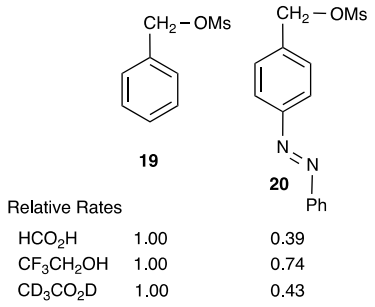

Figure 5. Relative solvolysis rates of benzylic systems.

retarding factor that ranges from 1.35 to 2.56 compared to the unsubstituted benzyl mesylate **19**. This contrasts with the phenylazo effect in the corresponding cumyl system, **13**, where the phenylazo group retards the rate by a somewhat larger factor of 5.2.

M062X/6-311+G** computational studies (Figure 6) have located the planar cation **22** as an energy minimum. This cation is delocalized as in form **22b** (nitrenium ion -type stabilization). A second structure, the 90° rotated cation **23**, has also been located, and this structure is not a transition state but instead a separate energy minimum in the gas phase. This cation state lies only 2.3 kcal/mol above the planar cation **22**. The computational study suggests the increased importance of cation stabilization by the nitrogen nonbonding electrons relative to the N−N π-electrons as the amount of charge on C4 increases. The C4−N−N angle in **23** increases to 136° and is indicative of the increased importance of form **23b**, an immonium type cation.

The situation changes somewhat when acetic acid is employed as a computational solvent. The phenylazo plane of lowest energy cation **22** is now rotated 23° relative to the benzylic cation portion of the molecule. Additionally, the 90°-rotated cation **23** is no longer an energy minimum but instead a transition state with one imaginary frequency. This transition state **23** now lies only 1.8 kcal/mol above cation **22**. The potential-energy surfaces in the gas phase, as well as in acetic acid, are therefore very flat with very small barriers to rotation. The computational study in acetic acid suggests a single energy minimum, while in the gas phase there are two energy minima. What is clear is that rotation in the cation involved in the solvolysis of mesylate **20** is a very facile process.

The behavior of the *cis*-phenylazo isomer **26** was also of interest. Irradiating the *trans*-alcohol **24** in a number of solvents leads (Scheme 4) to a photostationary state where the *cis*-alcohol **25** predominates over the *trans*-alcohol **24**. The actual ratio of the two isomers depends on the initial concentration of **24**, with more dilute solutions leading to a larger fraction of **25**. This mixture was converted to the corresponding mesylates in the CH_2Cl_2 solvent in a standard fashion. The mesylate **26** is a very unstable substrate that cannot be isolated in a pure form since it decomposes upon complete solvent removal. However, spectra of **26** can be recorded if the solvent is not completely removed and the residue is rapidly dissolved in $CDCl_3$. Alternatively, *cis*-mesylate **26** can be prepared by the irradiation of the *trans*-isomer **20** in C_6D_6, $CDCl_3$, or even CD_3CO_2D. In solvents such as C_6D_6, *cis*-mesylate **26** rearranges back to the *trans*-isomer **20** in an autocatalytic reaction. This process can be circumvented if a small amount of 2,6-lutidine is added before irradiation. Under these conditions, the thermal rearrangement of **26** back to **20** is a very slow process (half-life of 123 h) at room temperature.

When dissolved in CD_3CO_2D, mesylate **26** reacts readily at room temperature to give a major product of the internal return, the less reactive *trans*-mesylate **20**. Also formed are the *trans*-acetate **27** and a smaller amount of the *cis*-acetate **28** (Scheme 5). Mesylate **26** is 41× more reactive than the *trans*-isomer **20** in CD_3CO_2D. These observations are in line with a mechanism where the ionization of **26** is followed by the facile internal return of the mesylate anion to form mesylate **20**. It is tempting to suggest that ionization initially leads to the *cis*-cation **29**, which can capture the solvent to give *cis*-acetate **28** or readily isomerize to the *trans*-cation **22**, which leads to **20** and **27**. Computational studies were used in an attempt to evaluate the properties of *cis*-cation **29**. While the observation of a small amount of the *cis*-acetate **28** does implicate *cis*-cation **29** as a very transient intermediate, computational studies failed to locate

https://dx.doi.org/10.1021/acs.joc.1c00140
J. Org. Chem. XXXX, XXX, XXX−XXX

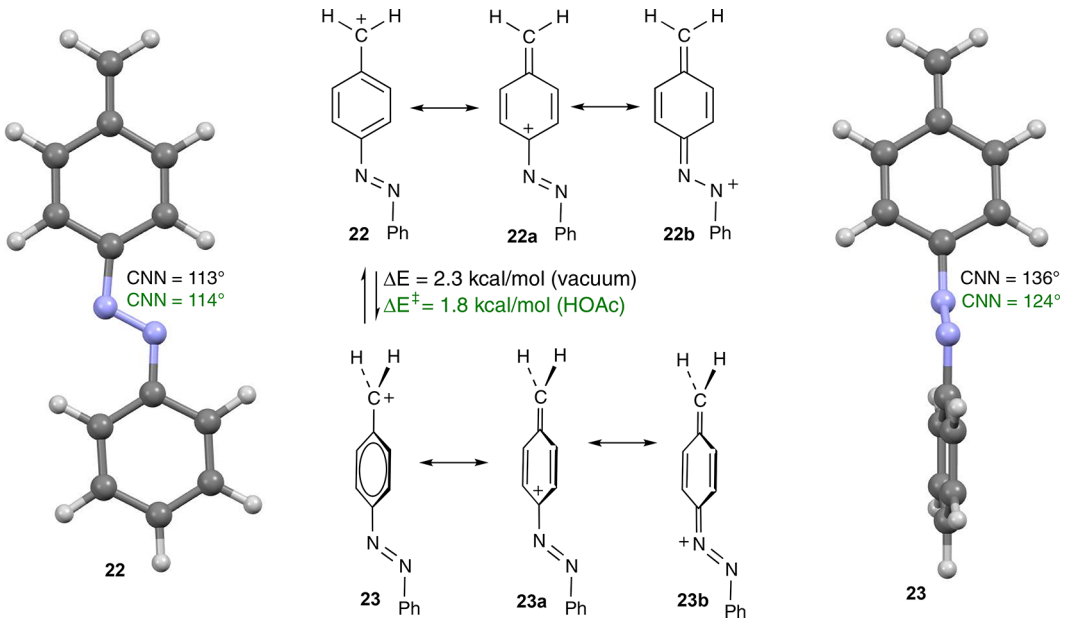

Figure 6. M062X/6-311+G**-calculated structures of benzylic cations **22** and **23**.

Scheme 4. Preparation of Mesylate 26

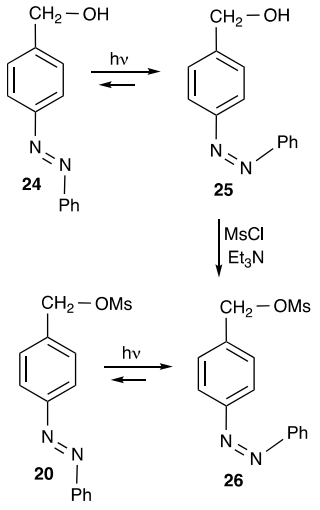

this cation as an energy minimum. All attempts to locate **29** resulted in a conversion to the *trans*-cation **22**.

Previous computational studies have been carried out on *cis*-azobenzene, **30**, and its substituted analogs in addition to the barrier to conversion to the more stable *trans*-analogs.[19] The conversion of the *cis*-azo compounds to their *trans*-analogs can occur by two reasonable mechanisms.[20] The first involves a rotation about the π-bond of the azo group. Such a transition state should have a biradical or dipolar character. A second possibility involves inversion at the sp^2-hybridized nitrogen center. It has been found that this inversion barrier decreases as the substituents on one of the phenyl groups become more electron-withdrawing. Our current M062X/6-311+G** calculations (Figure 7), which utilize acetic acid as a solvent, confirm this previous study,[19] which was carried out at the B3LYP/6-31G* level. The transition state for the conversion of the *cis*-azobenzene, **30**, to the *trans*-azobenzene, **36**, lies 29.0 kcal/mol above that of **30**. This value drops to 23.6 kcal/mol in the aldehyde **31**. What are the inversion barriers in cationic systems? In the stabilized benzylic cation **32** (a protonated imine), the barrier is further reduced to 13.4 kcal/mol. The values for the methoxy-substituted cation **33** and the α-CH_3 benzylic cation **34** drop to 8.1 and 1.3 kcal/mol, respectively, suggesting that the inversion of cations **32**−**34** should occur rapidly at room temperature. The reason for this decrease in the inversion barrier has been suggested[19] to involve the increased importance of forms such as **38a** (Figure 8) in the transition state. In other words, as C4 of the substituted phenyl group becomes more electron deficient, the interaction with the nitrogen nonbonding electrons increases. *cis*-Cations that are less stable than **34** (e.g., the cation **29**) could not be located as energy minima. Computationally, they revert to the *trans*-cations. On the basis of this systematic lowering of the isomerization barrier as the C4 carbon becomes more electron deficient, it is not surprising that benzylic cation **29** cannot be located as an energy minimum. This computational study suggests that there is no barrier for the conversion of **29** to the *trans*-isomer **22**.

***α*-Trifluoromethyl Benzyl Cations.** Can the phenylazo group become stabilizing in a benzylic-type cation? Can nitrogen nonbonding electron stabilization surpass N−N π-stabilization in such cations? In an attempt to induce such behavior, the demand for cation stabilization was further increased by the inclusion of the trifluoromethyl group into the benzylic cation. Thus, the ketone **46** was prepared (Scheme 6) by the trifluoroacetylation of the organolithium reagent derived from the iodide **45**.[21] The borohydride reduction of ketone **46** gave the alcohol **47**, which in turn was converted to the desired triflate **48**.

The rate of reaction of triflate **48** in CD_3CO_2D, where the corresponding acetate product was formed, was examined (Table 1). Triflate **48** was found to be 7.8× *more reactive* than the corresponding unsubstituted triflate **49** (Figure 9). In trifluoroethanol, this increased reactivity of **48** was a factor of 12.1. This is consistent with stabilization of the cationic intermediate by the phenylazo group. This contrasts with the behaviors in the substituted cumyl chloride **13** and the benzylic mesylate **20**, where the phenylazo effect is rate retarding. While this cation-stabilizing rate effect is interesting, it does not allow

https://dx.doi.org/10.1021/acs.joc.1c00140
J. Org. Chem. XXXX, XXX, XXX−XXX

Scheme 5. Reaction of Mesylate 26 in CD_3CO_2D

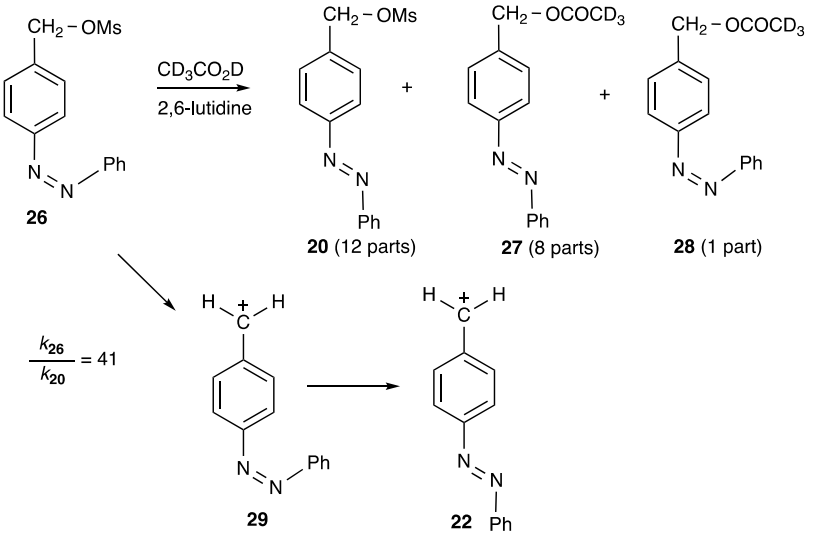

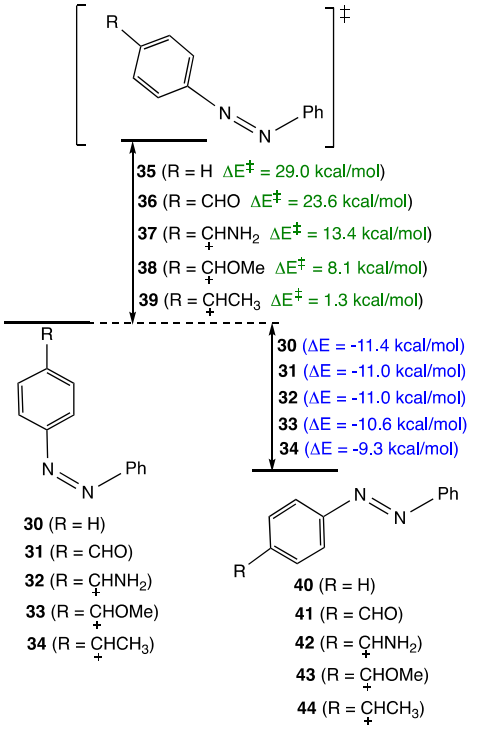

Figure 7. M062X/6-311+G**-calculated barriers in HOAc for inversion in *cis*-azobenzenes.

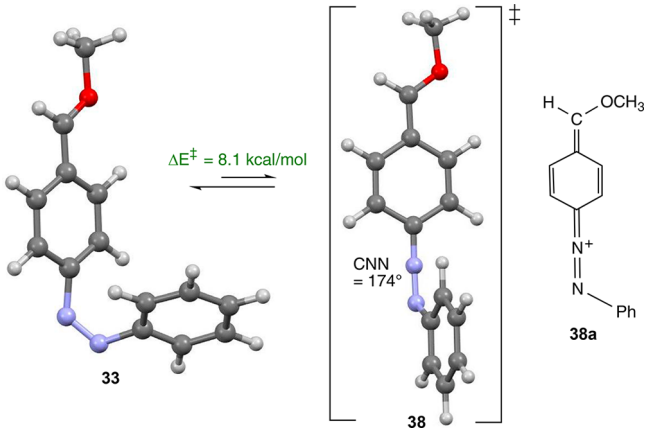

Figure 8. M062X/6-311+G**-calculated structures of the *cis*-azo cation **33** and the transition state **38**.

Scheme 6. Preparation of Triflate 48

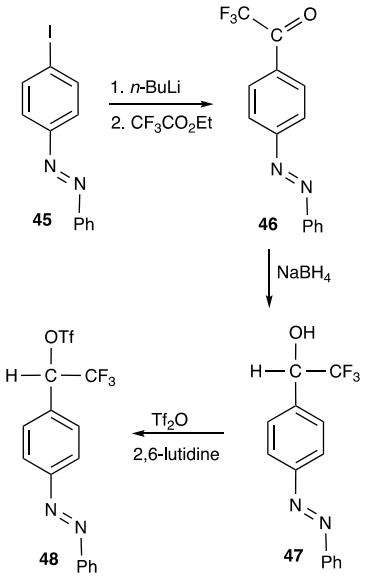

one to decide on the mode of the azo stabilization of the cationic intermediate.

A computational study was carried out on α-CF_3-substituted cations **50** and **51**, where the CF_3 group should increase the charge delocalization to C4. Both cations are energy minima in the gas phase and acetic acid. Scheme 7 shows that cation **50** and the rotated cation **51** differ by only 0.6 kcal/mol in the gas phase. In an acetic acid solvent, cation **50** is not completely planar. Instead, the phenylazo plane is rotated 14° relative to the other aryl ring. The rotated cation **51** in acetic acid is actually 1.0 kcal/mol lower in energy than **50**. The cation **50**, which is stabilized by the N–N π-bond (nitrenium ion-type stabilization), and the rotated cation cation **51** (immonium ion-type stabilization) are therefore of comparable energies. Of interest is the C–N–N bond angle in **51** that increased to 152° (162° in HOAc), which is indicative of the increased interaction of the nitrogen

https://dx.doi.org/10.1021/acs.joc.1c00140
J. Org. Chem. XXXX, XXX, XXX–XXX

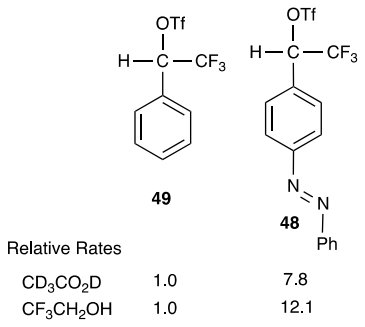

Figure 9. Relative solvolysis rates of α-CF_3-substituted benzylic systems.

nonbonding electrons with the electron-deficient C4. The structure **51** becomes more "allene like" as the nitrogen becomes more sp hybrid in character. The transition state **52** for the interconversion of these isomers has been located and is only 1.3 kcal/mol above **50** (0.7 kcal/mol in HOAc). The potential-energy surface is therefore quite flat and indicative of the facile interconversion of **50** and **51**. It is therefore quite probable that both cations are involved in the solvolysis of triflate **48**.

The 2-(Phenylazo)propyl Cation. Attention was next focused on the cations of general structure **12**, where the phenylazo group is attached directly to the cationic center. The cation **54** was previously generated under Lewis acid conditions and can effectively alkylate toluene.[16a] This cation has now been generated from the chloride **53** under solvolytic conditions in a variety of solvents. The behavior of **53** in CD_3CO_2D is quite revealing. When buffered with 2,6-lutidine, **53** rapidly forms the acetate substitution product **55** in CD_3CO_2D in a reaction that is essentially complete after 30 min at room temperature (Scheme 8). However, the disappearance of **53** is not strictly first order, i.e., the apparent first-order rate constant decreases as the reaction progresses (Figure S23). This is indicative of a common ion rate suppression. Indeed, when 0.1 M tetramethylammonium chloride is added at the beginning of the reaction, the rate of the reaction is greatly suppressed. When no buffering base is added to the CD_3CO_2D, **53** does not react completely. The reaction reaches an equilibrium position containing both **53** and the acetate **55** in amounts that depend on the starting concentration of **53**. This behavior provides classic evidence for the involvement of a relatively stable cationic intermediate **54** that lives long enough in the solution to reach the dissociated ion-pair stage. Externally added chloride ion can trap the intermediate **54** and thereby return it to the starting chloride **53**.

The reaction of **53** in CD_3OD containing 0.0646 M sodium azide at room temperature (Scheme 8) supports the suggestion of a relatively stable cationic intermediate **54**. Jencks and Richard have used this method to estimate carbocation lifetimes in solution.[22,23b] Under these conditions, the azide **56** was the predominant product formed (88%), while only 12% of the solvent capture product **57** was formed. Apparently, methanol reacts with cation **54** rather slowly (relative to the azide ion). Since this product ratio (88:12) should equal the ratio of $k_{azide}[NaN_3]/k_{CD3OD}$, these data allow one to calculate the value of k_{azide}/k_{CD3OD}. This value of k_{azide}/k_{CD3OD} is 114 M^{-1}. Since k_{azide} is close to the diffusion-controlled limit[23] of 5×10^9 M^{-1} s^{-1}, k_{CD3OD} is significantly smaller than the diffusion controlled limit. In other words, cation **54** has an appreciable lifetime in pure CD_3OD. By way of contrast, the k_{azide}/k_{CH3OH} value is 0.67 M^{-1} for the solvolysis of cumyl chloride **58** under the same conditions. This suggests that the 3° benzylic cumyl cation **17** is much shorter lived than cation **54**.

Scheme 7. M062X/6-311+G-Calculated Interconversion of Cations 50 and 51 via Transition State 52**

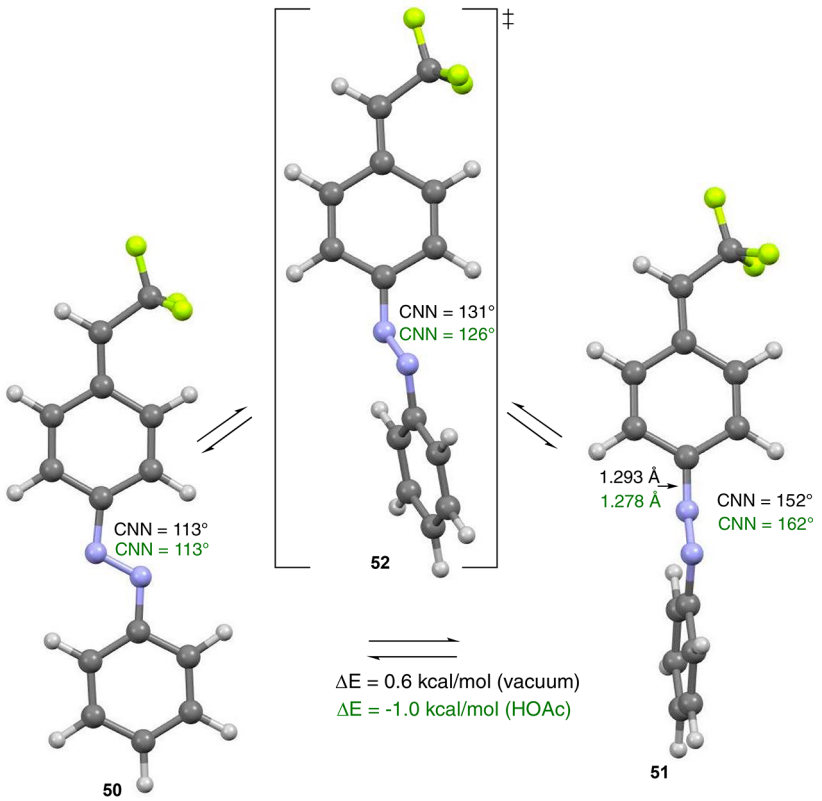

https://dx.doi.org/10.1021/acs.joc.1c00140
J. Org. Chem. XXXX, XXX, XXX−XXX

Scheme 8. Reactions of Chloride 53 in CD_3CO_2D and CD_3OD with Added NaN_3

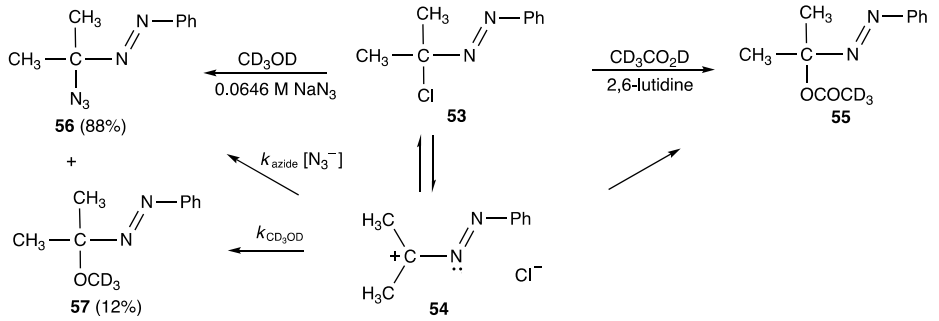

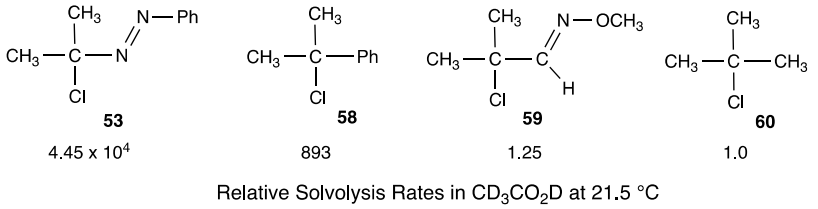

Figure 10. Relative solvolysis rates of **53** and its substituted analogs.

Scheme 9. M062X/6-311+G-Calculated Isodesmic Reaction of Cation 54 with Isobutane**

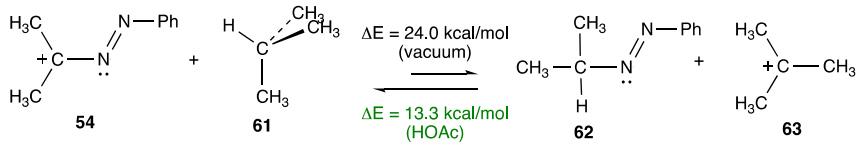

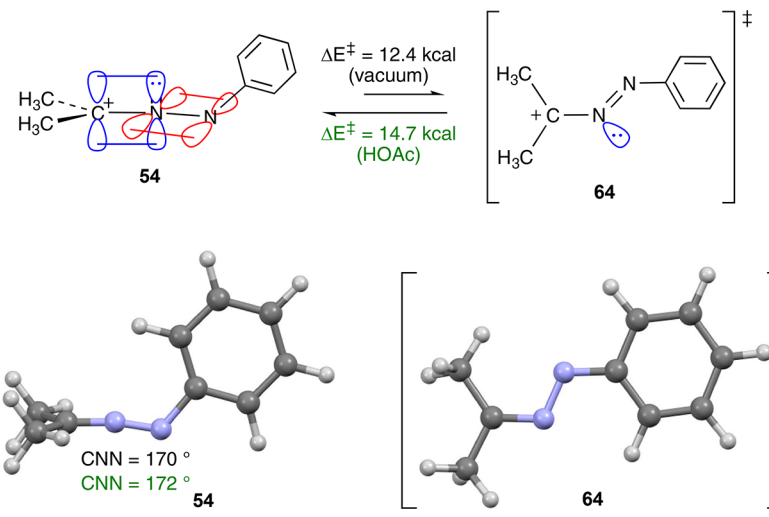

Figure 11. M062X/6-311+G**-calculated structures of cation **54** and transition state **64**.

How does the rate of solvolysis of chloride **53** compare with those of other chlorides? For comparison purposes, rate data were obtained for the chlorides **58**–**60** (Table 1) and are summarized in Figure 10. Because of the common ion rate suppression during the acetolysis of **53**, the rate given in Table 1 represents an initial rate. This initial rate was determined by rapidly mixing CD_3CO_2D (containing buffering 2,6-lutidine) with **53** and then rapidly quenching portions of this solution in C_6D_6 prior to ^1H NMR analysis. The rate constant in Table 1 represents a value determined from the first 20 seconds of the reaction (Figure S25). A comparison of the rate of **53** with these substrates shows that the phenylazo group greatly enhances the rate when attached directly to a developing cationic center. The acetolysis rate of **53** is 44 500× faster than that of *t*-butyl chloride, **60**, and also exceeds that of cumyl chloride, **58**. These data suggest that the cation-stabilizing ability of the phenylazo group greatly exceeds those of the methyl group and the phenyl group. Of interest is the observation that the phenylazo group of **53** is substantially more cation-stabilizing than the oxime functional group in **59** (a group that is cation-stabilizing via a π-conjugative effect).[12] These relative rate comparisons also lead to the conclusion that the cationic intermediate **54**, derived from acetolysis of **53**, is highly stabilized.

https://dx.doi.org/10.1021/acs.joc.1c00140
J. Org. Chem. XXXX, XXX, XXX−XXX

Computational studies (M062X/6-311+G**) were used to further sort out the structure and energetics of cation **53**. The isodesmic reaction shown in Scheme 9 allows a comparison with *t*-butyl cation **63**, i.e., a comparison of the cation-stabilizing ability of the methyl group vs the phenylazo group. This calculation suggests that **54** is significantly stabilized relative to the *t*-butyl cation, but the calculation is quite solvent dependent. The stabilization energy of 24 kcal/mol in the gas phase drops to 13.3 kcal/mol when acetic acid (used for the solvolytic studies in Figure 10) is included as the solvent when using the polarizable continuum model.

As is expected based on the previously calculated structure of **54**,[24] as well as a dialkyl-α-phenylazo cation,[16a] our calculated structure of cation **54** shown in Figure 11 indicates that stabilization is due to the nitrogen nonbonding electrons. In valence-bond terms, the C−N−N bond angle of 170° (172° in acetic acid) is in line with the central nitrogen being essentially sp hybridized due to the extensive interaction of the nitrogen nonbonding electrons with the cation vacant orbital. The planar form **64** is not an energy minimum but instead a transition state (one imaginary frequency) lying 12.4 kcal/mol (14.7 kcal/mol in acetic acid) above **54**. These calculations imply that as the charge increases at the cationic center, the nitrogen nonbonding electron pair becomes a more effective cation stabilizer.

Computationally, how does the azo group compare with other cation stabilizers and destabilizers? Figure 12 shows M062X/6-311+G**-calculated stabilization energies of cations relative to the *t*-butyl cation (R = CH_3) using isodesmic reactions analogous to Scheme 9. Phenylazo stabilization, when directly attached to the cationic center of **65**, exceeds those of the *O*-methyl oxime group and the phenyl group. These computational studies are in line with the rate data in Figure 9, where the rate data parallel the calculated cation stabilization energies.

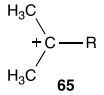

65

R =	−N=N−Ph	−Ph	−CH=N−OCH3	−CH3	−H	−CN
vacuum	24.0	15.0	9.3	***0.0***	-16.1	-32.6
HOAc	13.3	5.9	0.8	***0.0***	-12.7	-32.0

Figure 12. M062X/6-311+G**-calculated relative stabilization energies of cations **65** (kcal/mol).

γ-Silyl Substitution. Given the extraordinary cation-stabilizing properties of the phenylazo group directly attached to a carbocationic center, it was of interest to determine if this group could offset the stabilization of other potent cation stabilizers. Our studies,[25] and those of others,[26] have shown that the γ-trimethylsilyl group can be a potent cation-stabilizing group. The γ-trimethylsilyl cation **69** (or **70**) was therefore chosen for study. Is this cation stabilized by the γ-trimethylsilyl group or has this remote stabilization been "wiped out" by the phenylazo group? What is the geometry of the phenylazo group with respect to the R_2C^+ plane (perpendicular as in **54** or planar as in **64**)? The azo compounds **67** and **68** were therefore prepared (Scheme 10) as a mixture of isomers by the oxidation of the hydrazone **66**.

The reaction of this mixture of chlorides **67** and **68** at room temperature in CH_3CO_2H gave the acetates **71a** and **72a** as a 69:31 mixture of isomers (Scheme 11). In CH_3OH, ethers **71b** and **72b** were formed in a 73:27 ratio. Both **67** and **68** reacted at comparable rates in CD_3CO_2D. However, as in the case of chloride **53**, there was a common ion rate suppression during acetolysis, which complicated the determination of first-order rate constants. The formation of the product mixtures **71** and **72** is indicative of the involvement of a classical cationic intermediate **69**, which is not stabilized by the γ-trimethylsilyl group. This cation can capture the solvent from the bottom as well as from the top. The nonclassical bicyclobutonium-type cation **70** is not involved. If such a cation, **70**, were involved, then the expected products would be exclusively the acetate **71a** or the methyl ether **71b**. This is based on our previous studies[25] that show that nonclassical 3-trimethylsilylcyclobutyl cations **73**, which contain a wide variety of R groups ranging from H, to CH_3 to Ar, all capture the solvent exclusively from the bottom side to give only products **74**.

Scheme 10. Preparation of Chlorides 67 and 68

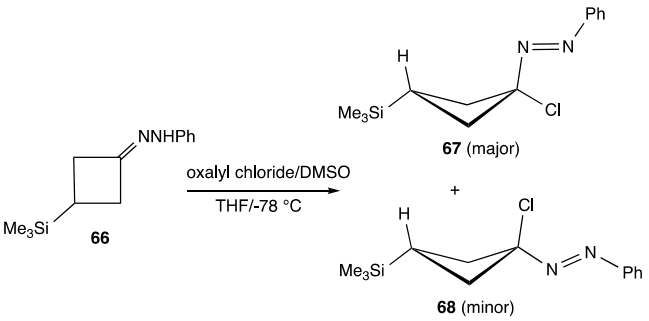

Computational studies are in line with the conclusion that cation **69** is a classical cation that does not involve γ-trimethylsilyl stabilization. Figure 13 shows the calculated structure of cation **69**. The cross-ring C1−C3 bond distance is 2.095 Å, which indicates no significant cross-ring interaction with the rear lobe of the C3−Si bond. The C3−Si bond length is 1.910 Å, which is expected for a "normal" carbon−silicon bond. The stabilization of **69** is of the "immonium" type as in structure **69a**, which is evidenced by the 169 °CNN angle. This type of stabilization in **69a** is apparently enough to offset potential bicyclobutonium-like stabilization as well as the cross-ring γ-trimethylsilyl stabilization shown in **70**.

Further Computational Studies. Do α-phenylazo-substituted carbocations ever exist preferentially in the planar (π-stabilized) form? M062X/6-311+G** computational studies were carried out to provide further insight. The formally aromatic cations **75**−**77** (Figure 14) were examined, since these highly stabilized cations should have a reduced demand for phenylazo stabilization. Indeed, cations **75a** and **76a** are planar energy minima in the gas phase. The conformations of **75a** and **76a**, with the azo group rotated 90° from the plane of the aromatic cation rings, are transition states lying only 2.5 and 4.5 kcal/mol above **75a** and **76a**, respectively. The phenylazo group in cation **77a** is slightly twisted out of planarity by 22° with the cycloheptatrienyl ring. The perpendicular conformation of **78** is a transition state 4.2 kcal/mol above **77a**. These studies show that the N−N π-bond of the phenylazo group will indeed align in conjugation with a cationic center as long as the demand for cation stabilization is not too large. The situation was slightly different when the calculation was carried out in acetic acid. Cation **76b** is no longer planar, but the aromatic pyranyl portion of the cation is slightly twisted (16°) out of conjugation with the phenylazo group. Further twisting was also observed for cation **77b**, which was rotated by 29° in acetic acid.

https://dx.doi.org/10.1021/acs.joc.1c00140
J. Org. Chem. XXXX, XXX, XXX−XXX

Scheme 11. Reaction of Chlorides 67 and 68 in CH_3CO_2H and CH_3OH

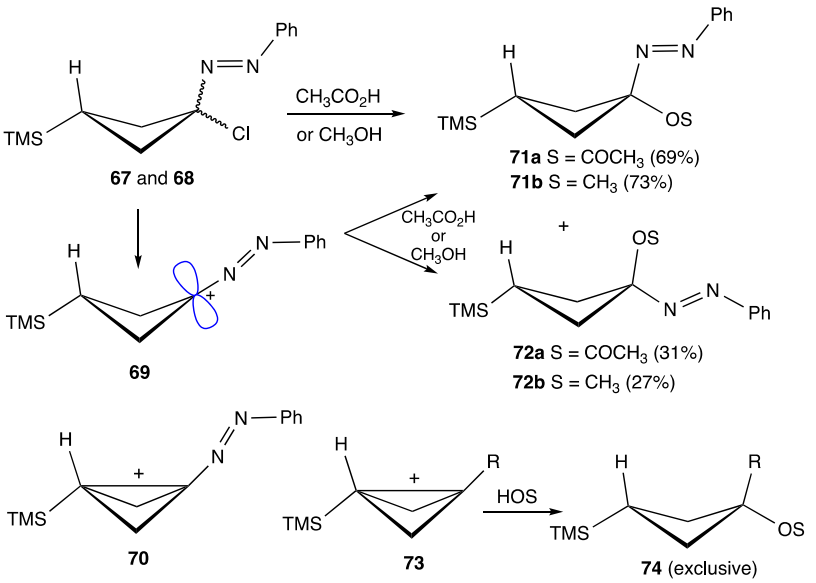

23

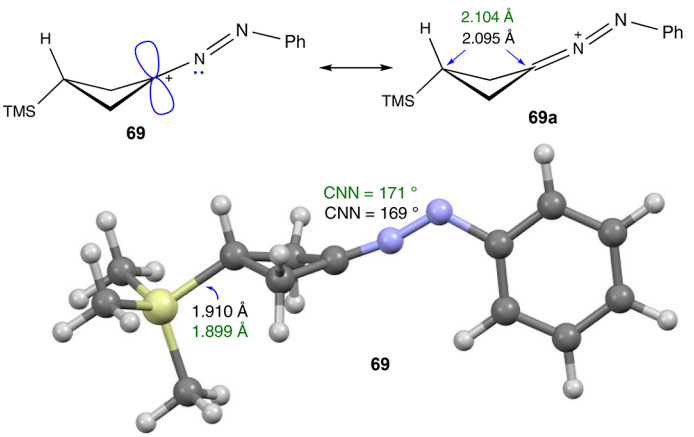

Figure 13. M062X/6-311+G**-calculated structure of cation **69**.

The methoxy group in cation **79** is also stabilizing enough that the planar form of the cation is the lowest-energy conformation (Figure 15). A second energy minimum, cation **80**, could be located where the phenylazo group is rotated 28° (32° in HOAc) out of conjugation with the cationic center. This conformation of **80** is in line with stabilizing interactions with *both* the nitrogen nonbonding electrons and the N−N π-bond (since neither of these orbitals are orthogonal to the vacant p-orbital at the cationic center). Unlike the methoxy group, the phenyl group does not offer sufficient stabilization in cation **81**, and this planar conformation is no longer the lowest energy. The rotated allene-like conformation **82** now becomes the lowest-energy minimum in both the gas phase and the acetic acid solvent.

CONCLUSIONS

Computational studies show that there are two different modes by which the phenylazo group can stabilize an electron-deficient carbon center. The first mode involves an interaction with the N−N π-bond. This involves charge delocalization from the carbon to the second nitrogen atom, which imparts a nitrenium ion character to this nitrogen. This type of delocalization manifests when the phenylazo group is in the *para*-position of cumyl and benzylic cations **14** and **22**, respectively. Based on the experimental rates of formation of cations **14** and **22**, the phenylazo group behaves as a net electron-withdrawing group. This N−N π-stabilization is therefore a weak stabilizing effect that barely offsets the inductive effect of the azo group. The second stabilization mode involves the interaction of a carbon with the adjacent nitrogen nonbonding electrons and imparts an immonium ion character to the adjacent nitrogen. This stabilization mode becomes competitive with the π-stabilization mode in the α-CF_3-substituted benzylic cations **50** and **51**, where the demand for stabilization is increased. Experimentally, cations **50** and **51** are formed more readily than the unsubstituted cation $[PhCHCF_3]^+$, indicating that the phenylazo group is now a weak electron-donor group. The phenylazo group becomes a potent electron-donor group in cation **54** $[Me_2C—N{=}N—Ph]^+$, where stabilization involves the nitrogen nonbonding electrons. The cation **54** is relatively stable and lives long enough in a methanol solution to be effectively trapped by externally added azide ion. Thus, with the increased demand, nitrogen nonbonding electron stabilization is more potent than N−N π-stabilization and is even strong enough to

https://dx.doi.org/10.1021/acs.joc.1c00140
J. Org. Chem. XXXX, XXX, XXX−XXX

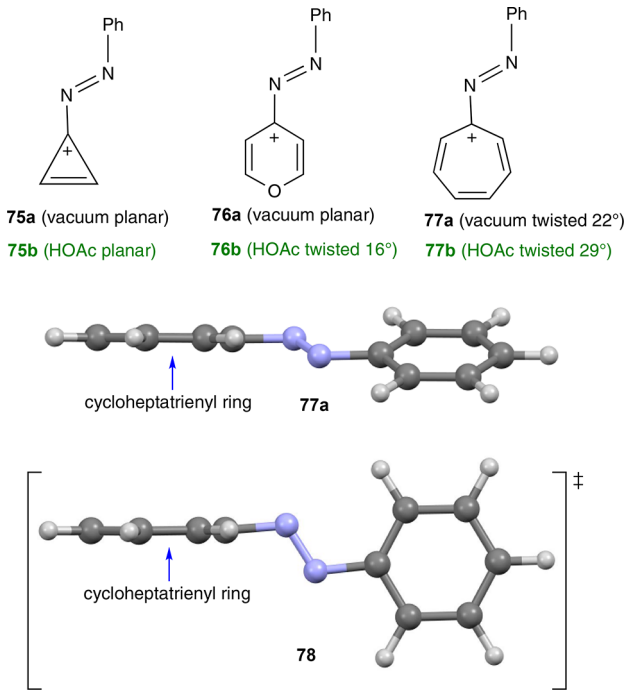

Figure 14. M062X/6-311+G**-calculated structures of cations **74**–**77** and transition state **77**.

offset potential γ-silyl stabilization in the cation **69**. However, in the aromatic cations **75**–**77**, the demand for cation stabilization is quite low. Hence, stabilization reverts back to the less effective N–N π-stabilization.

The unusual *cis*-phenylazo mesylate **26** reacts much faster than the *trans*-mesylate **20** under solvolytic conditions. The products formed in acetic acid-d_4 are mostly rearranged to *trans*-isomers. They are in line with a stepwise ionization, cation isomerization, and nucleophile capture mechanism for *cis*-mesylate **26**. Computational studies suggest, however, that no barrier exists for the isomerization of the *cis*-phenylazo cation **29** to the *trans*-phenylazo cation **22**.

EXPERIMENTAL SECTION

General. NMR spectra were recorded on a Varian DirectDrive 600 MHz spectrometer. HRMS measurements were carried out using a Bruker MicroTOF-II spectrometer (electrospray ionization source with time-of-flight mass analyzer).

Preparation of *trans*-4-Phenylazobenzyl Mesylate (20). To 4-phenylazobenzyl alcohol[27] (67.4 mg, 0.318 mmol) partially dissolved in 3 mL of CH_2Cl_2 was added 48.3 mg (0.422 mmol) of mesyl chloride. The solution was cooled in an ice/salt bath at −10 °C, and 53.8 mg (0.533 mmol) of Et_3N in about 1.0 mL of CH_2Cl_2 was added dropwise. The mixture was warmed to room temperature and then taken up into 5 mL of ether. Then, 3 mL of pentane was added. The solution was consecutively washed with cold water, a cold dilute HCl solution, cold water, a $NaHCO_3$ solution, and a saturated NaCl solution and then dried over a mixture of Na_2SO_4 and $MgSO_4$. After filtration, the solvent was removed using a rotary evaporator to give 88.3 mg (96% yield) of the mesylate as an orange solid, mp >95 °C (dec). The mesylate discolors upon standing at room temp. It was stored in an ether solution at −20 °C. Mesylate **20** gave no parent peak during the attempted HRMS analysis. ^{1}H NMR of **20** (600 MHz, $CDCl_3$): δ 7.98–7.91 (m, 4 H), 7.58 (d, J = 8.5 Hz, 2 H), 7.56–7.48 (m, 3 H), 5.32 (s, 2 H), 2.97 (s, 3 H). ^{13}C{^{1}H} NMR of **20** (150 MHz, $CDCl_3$): δ 153.0, 152.5, 135.9, 131.4, 129.5, 129.2, 123.3, 123.0, 70.7, 38.5.

Preparation of *cis*-4-Phenylazobenzyl Alcohol (25). *trans*-4-Phenylazobenzyl alcohol, **24** (27 mg), was dissolved in 7 mL of C_6H_6. The solution was irradiated in a Rayonet Photochemical Reactor using 350 nm bulbs for 100 min. The C_6H_6 was removed at approximately a 30 mm pressure using a water aspirator. NMR analysis showed a mixture containing 85% *cis*-4-phenylazobenzyl alcohol, **25**, and 15% *trans*-4-phenylazobenzyl alcohol, **24**. ^{1}H NMR of **25** (600 MHz, $CDCl_3$): δ 7.15 (t, J = 7.3 Hz, 4 H), 7.05 (t, J = 7.3 Hz, 1 H), 6.73 (d, J = 8.3 Hz, 4 H), 4.53 (s, 2 H). ^{13}C{^{1}H} NMR of **25** (150 MHz, $CDCl_3$): δ 153.4, 152.5, 140.2, 128.8, 127.2, 120.9, 120.4, 64.6. HRMS (ESI): m/z $(M + H)^+$ calculated for $C_{13}H_{13}N_2O$ 213.1022, found 213.1024.

Preparation of *cis*-4-Phenylazobenzyl Mesylate (26). A mixture of 22 mg of the alcohols **24** and **25** (0.104 mmol; 70% *cis*-alcohol **25**) in 2 mL of CH_2Cl_2 was cooled to −10 °C, and 30 mg of CH_3SO_2Cl (0.262 mmol) in 0.2 mL of CH_2Cl_2 was added. Then, a solution of 40 mg of Et_3N (0.396 mmol) in 0.2 mL of CH_2Cl_2 was added dropwise. The mixture was warmed to about 10 °C and then transferred to a separatory funnel. Pentane (8 mL) was then added, and the mixture was extracted with cold water, a cold dilute HCl solution, cold water, a $NaHCO_3$ solution, and a saturated NaCl solution. After drying over a mixture of Na_2SO_4 and $MgSO_4$, the solution was stored at −20 °C. Mesylate **26** readily decomposed upon complete solvent

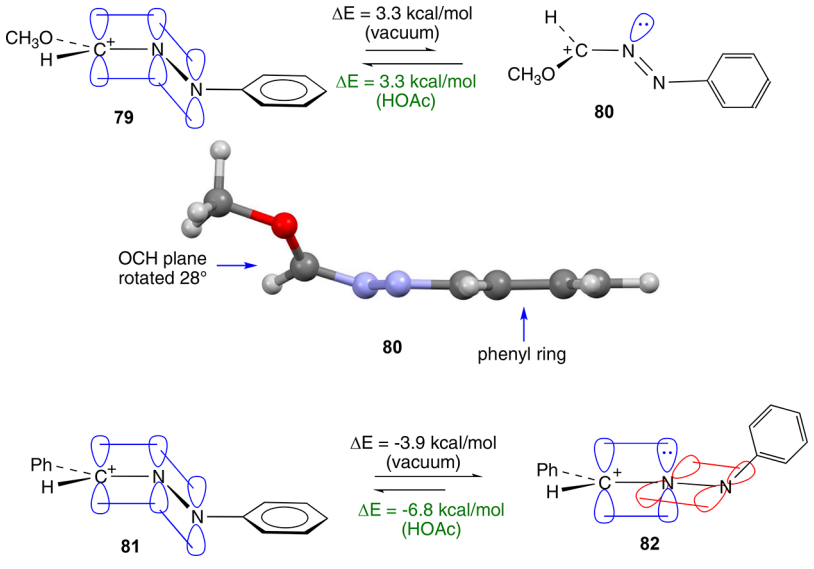

Figure 15. M062X/6-311+G**-calculated structures of cations **79**–**82**.

https://dx.doi.org/10.1021/acs.joc.1c00140
J. Org. Chem. XXXX, XXX, XXX–XXX

removal. The solvent was partially removed from a solution of mesylate **26** in CH_2Cl_2/pentane using a rotary evaporator and cooling in ice. The residue was rapidly dissolved in $CDCl_3$, and spectra were recorded at 0 °C. Even at this temperature, *cis*-mesylate **26** rearranged to *trans*-mesylate **20**.

Alternatively, *cis*-mesylate **26** can be prepared in a $CDCl_3$ solution by the irradiation of *trans*-mesylate **20** in the presence of 2,6-lutidine. Thus, a solution of 3.2 mg of mesylate **20** in 4 mL of $CDCl_3$ containing approximately 1.5 mg of 2,6-lutidine was irradiated for 10 min in a Rayonet Photochemical Reactor using 350 nm bulbs. The volume was then reduced to about 1 mL using a rotary evaporator, and NMR spectra showed mesylates **26** and **20** in a 75:25 ratio. Mesylate **26** gave no parent peak during the attempted HRMS analysis. ^{1}H NMR of **26** (600 MHz, $CDCl_3$): δ 7.31 (d, J = 8.2 Hz, 2 H), 7.25 (t, J = 7.6 Hz, 2 H), 7.16 (t, J = 7.5 Hz, 1 H), 6.87 (d, J = 8.2 Hz, 2 H), 6.83 (d, J = 8.2 Hz, 2 H), 5.17 (s, 2 H), 2.89 (s, 3 H). ^{13}C{^{1}H} NMR of **47** (150 MHz, $CDCl_3$): δ 154.1, 153.2, 132.3, 129.3, 128.8, 127.7, 120.9, 120.5, 70.6, 38.4.

cis-Mesylate **26** can also be prepared in CD_3CO_2D *in situ* by the irradiation of *trans*-mesylate **20**. Thus, a solution of 1.0 mg of CD_3CO_2Na in 1.028 g of CD_3CO_2D was added to 1.0 mg of mesylate **20**. A portion of this solution was irradiated in a 3 mm NMR tube for 6 min. Immediate ^{1}H NMR analysis showed mesylates **26** and **20** in a 75:25 ratio. ^{1}H NMR of **26** (600 MHz, CD_3CO_2D): δ 7.37 (d, J = 8.32 Hz, 2 H), 7.28 (t, J = 7.6 Hz, 2 H), 7.19 (t, J = 7.5 Hz, 2 H), 6.94 (d, J = 8.3 Hz, 2 H), 6.89 (d, J = 8.0 Hz, 2 H), 5.18 (s, 2 H), 2.96 (s, 3 H). This solution was immediately used for a kinetic study.

Preparation of Ketone 46. Using the previously described procedure for the preparation of 4-lithioazobenzene,[28] 4-iodoazobenzene, **45**[29] (604 mg, 1.960 mmol) was dissolved in 35 mL of ether under nitrogen, and the stirred mixture was cooled to −78 °C. Some of the iodide **45** comes out of solution at this temperature. *n*-Butyllithium (1.4 mL of 1.6 M in hexanes, 2.240 mmol) was added dropwise via syringe. The mixture was stirred at −78 °C for 3 h and then slowly warmed to −30 °C. The mixture was cooled to −78 °C, and a solution of 420 mg of ethyl trifluoroacetate (2.956 mmol) in 7 mL of ether was slowly added dropwise. The mixture was stirred for 1 h at −78 °C and then slowly warmed to −20 °C. The reaction was then quenched with water. After the ice melted, the mixture was transferred to a separatory funnel. The ether phase was washed with water and a saturated NaCl solution and then dried over a mixture of Na_2SO_4 and $MgSO_4$. After filtration, about 3 g of silica gel was added to the ether solution, and the solvent was removed using a rotary evaporator. The dry powder was then added to a column prepared from 10 g of silica gel packed with 1% ether in pentane. The column was eluted with increasing amounts of ether in pentane. The ketone **46** eluted with 4−6% ether in pentane. Solvent removal gave 180 mg (33% yield) of ketone **46** as a red-orange solid, mp 77−78 °C. ^{1}H NMR of **46** (600 MHz, $CDCl_3$): δ 8.25 (d, J = 8.7 Hz, 2 H), 8.04 (d, J = 8.7 Hz, 2 H), 8.01−7.96 (m, 2 H), 7.59−7.53 (m, 3 H). ^{13}C{^{1}H} NMR of **46** (150 MHz, $CDCl_3$): δ 180.0 (q, $^2J_{CF}$ = 36 Hz), 156.2, 152.5, 132.4, 131.4 (q, $^3J_{CF}$ = 2.4 Hz), 131.0, 129.3, 123.4, 123.3, 116.7 (q, $^1J_{CF}$ = 191 Hz). HRMS (ESI): m/z (M + H)$^+$ calculated for $C_{14}H_{10}F_3N_2O$ 279.0740, found 279.0741.

Preparation of Alcohol 47. A solution of 140 mg (0.503 mmol) of 4-trifluoroacetylazobenzene, **46**, in 3 mL of methanol was cooled in a water bath, and 100 μL of 0.6 M $NaOCH_3$ in methanol was added. Sodium borohydride (94 mg, 2.485 mmol) was added in small portions to the mixture, and stirring continued for 30 min. About 12 mL of ether was added, and the mixture was carefully quenched by the addition of 10 mL of 1% HCl in water. The aqueous phase was separated, and the ether extract was washed with water and a saturated NaCl solution. The ether extract was dried over a mixture of Na_2SO_4 and $MgSO_4$ and filtered, and the solvent was removed using a rotary evaporator to give 138 mg of the crude product **47**. This crude product was dissolved in 4 mL of ether, and 1.3 g of silica gel was added to the ether solution. The solvent was removed using a rotary evaporator, and the dry powder was then added to a column prepared from 6 g of silica gel and packed with 5% ether in pentane. The column was eluted with increasing amounts of ether in pentane. The product **47** (129 mg, 91% yield) eluted with 15−20% ether in pentane as an orange solid, mp 95−96 °C. ^{1}H NMR of **47** (600 MHz, $CDCl_3$): δ 7.97−7.91 (m, 4 H), 7.64 (d, J = 8.5 Hz, 2 H), 7.56−7.48 (m, 3 H), 5.12 (m, 1 H), 2.74 (d, J = 4.2 Hz, 1 H). ^{13}C{^{1}H} NMR of **47** (150 MHz, $CDCl_3$): δ 153.2, 152.6, 136.3, 131.4, 129.2, 128.3, 124.0 (q, $^1J_{CF}$ = 282 Hz), 123.00, 122.96, 72.5 (q, $^2J_{CF}$ = 32 Hz). HRMS (ESI): m/z (M + H)$^+$ calculated for $C_{14}H_{12}F_3N_2O$ 281.0896, found 281.0893.

Preparation of Triflate 48. A solution of 63 mg (0.225 mmol) of alcohol **47** in 1.0 mL of CH_2Cl_2 was stirred, and 54 mg (0.505 mmol) of 2,6-lutidine in 1.0 mL of CH_2Cl_2 was added. The mixture was cooled to −10 °C, and a solution of 122 mg of triflic anhydride (0.433 mmol) in 0.6 mL of CH_2Cl_2 was then added dropwise at −10 °C. The mixture was warmed to 0 °C and then transferred to a separatory funnel using 3 mL of ether. Pentane (6 mL) was then added, and the mixture was rapidly extracted with cold water, a dilute HCL solution, cold water, a $NaHCO_3$ solution, and a saturated NaCl solution. The organic extract was dried over a mixture of Na_2SO_4 and $MgSO_4$ and filtered, and solvents were removed using a rotary evaporator to give 82 mg (88% yield) of triflate **48** as an orange solid that decomposed when heated above 80 °C. Triflate **48** was stored in an ether solution at −20 °C. Triflate **48** gave no parent peak during the attempted HRMS analysis. ^{1}H NMR of **48** (600 MHz, $CDCl_3$): δ 8.01 (d, J = 8.5 Hz, 2 H), 7.97−7.92 (m, 2 H), 7.66 (d, J = 8.3 Hz, 2 H), 7.57−7.51 (m, 3 H), 5.93 (q, J = 5.8 Hz, 1 H). ^{13}C{^{1}H} NMR of **48** (150 MHz, $CDCl_3$): δ 154.3, 152.4, 131.9, 129.9, 129.2, 129.0, 123.5, 123.2, 121.4 (q, $^1J_{CF}$ = 280 Hz), 118.3 (q, $^1J_{CF}$ = 320 Hz), 82.1 (q, $^2J_{CF}$ = 36 Hz).

Preparation of Chloride 53. This substrate was prepared as previously described.[16a]

Reaction of Chloride 53 in CH_3CO_2H. To 28 mg (0.153 mmol) of chloride **53** was added a solution of 25 mg of 2,6-lutidine (0.234 mmol) in 3 mL of CH_3CO_2H, and the mixture was kept at room temperature for 130 min. The solution was transferred to a separatory funnel, and 6 mL of pentane was added, followed by 10 mL of water. The pentane extract was washed with two additional portions of water and then a $NaHCO_3$ solution. After being dried over Na_2SO_4, the pentane solvent was removed using a rotary evaporator, and the residue was filtered through 250 mg of silica gel in a pipet using 5% ether in pentane. Solvent removal gave 29 mg (92% yield) of the acetate **55** as a yellow oil. ^{1}H NMR (600 MHz, $CDCl_3$): δ 7.68 (m, 2 H), 7.48−7.41 (m, 3 H), 2.16 (s, 3 H), 1.68 (s, 6 H). ^{13}C{^{1}H} NMR (150 MHz, $CDCl_3$): δ 169.6, 151.57, 130.8, 129.0, 122.5, 101.6, 24.6, 22.1. HRMS (ESI): m/z (M + Na)$^+$ calculated for $C_{11}H_{14}N_2NaO_2$ 229.0947, found 229.0942.

Reaction of Chloride 53 in CH_3OH. Methanol (3.9 mL) was added to 19 mg of chloride **53**, and the mixture was kept at room temperature for 30 min. Then, sodium methoxide (0.2 mL of 0.6 M in methanol) was added. The methanol was removed using a rotary evaporator, and 4 mL of pentane was added to the residue. The mixture was washed with two portions of water, and the pentane extract was dried over Na_2SO_4. After the removal of the pentane using a rotary evaporator, the residue (15.8 mg) was filtered through 260 mg of silica gel in a pipet using 2% ether in pentane. Solvent removal gave 14.4 mg of the ether **57**-(OCH_3) as a yellow oil. ^{1}H NMR (600 MHz, $CDCl_3$): δ 7.73 (m, 2 H), 7.50−7.42 (m, 3 H), 3.51 (s, 3 H), 1.43 (s, 6 H). ^{13}C{^{1}H} NMR (150 MHz, $CDCl_3$): δ 151.7, 130.8, 129.0, 122.4, 98.3, 51.0, 23.4. HRMS (ESI): m/z (M + Na)$^+$ calculated for $C_{10}H_{14}N_2NaO$ 201.0998, found 201.0987.

Preparation of Azide 56. To a stirred solution of 30 mg of NaN_3 (0.461 mmol) in 2.0 mL of DMSO was added a solution of 14 mg of chloride **53** (0.077 mmol) in 100 μL of pentane dropwise. The mixture was stirred for 30 min and then transferred to a separatory funnel with 10 mL of water and 4 mL of pentane. The pentane extract was washed with two portions of water and then dried over Na_2SO_4. The solvent was removed using a rotary evaporator, and the residue was filtered through 200 mg of silica gel in a pipet using 2% ether in pentane. Solvent removal gave 7.6 mg (49% yield) of azide **56** as a yellow oil. ^{1}H NMR (600 MHz, $CDCl_3$): δ 7.60 (m, 2 H), 7.51−7.45 (m, 3 H), 1.58 (s, 6 H). ^{13}C{^{1}H} NMR (150 MHz, $CDCl_3$): δ 151.0, 131.3, 129.1, 122.7, 86.5, 24.4. HRMS (ESI) for the phenylacetylene triazole derivative:[30] m/z (M + H)$^+$ calculated for $C_{17}H_{18}N_5$ 292.1557, found 292.1553.

https://dx.doi.org/10.1021/acs.joc.1c00140
J. Org. Chem. XXXX, XXX, XXX−XXX

Preparation of Chlorides 67 and 68. Using a procedure analogous to the preparation of **53**, dimethyl sulfoxide (231 mg; 2.957 mmol) was dissolved in 8 mL of dry THF, and the mixture was cooled to −70 °C. To the stirred mixture was added oxalyl chloride (0.20 mL; approximately 296 mg; 2.332 mmol) via syringe over about 10 s at −70 °C. The mixture was stirred between −60° and −65 °C for 20 min and then cooled to −78 °C. To the stirred mixture was then added a solution of 450 mg (1.936 mmol) of the phenylhydrazone derivative of 3-trimethylsilylcyclohexanone and 300 mg (2.970 mmol) of Et_3N in about 5 mL of THF dropwise over 15 min. After 20 min at −78 °C, the mixture was allowed to warm to room temperature. Pentane (10 mL) was then added, and the mixture was filtered using a Buchner funnel to remove the Et_3NHCl. The salts were washed with an additional 5 mL of pentane. The clear orange solution was placed on a rotary evaporator to remove the solvents. The oily residue was extracted with 10 mL of pentane, and the orange pentane extract was filtered through a small amount of $MgSO_4$ in a pipet. The solvent was removed from the pentane solution, and the residue was chromatographed on a column prepared from 9.3 g of silica gel packed with 4% ether in pentane. The column was eluted with 4% ether in pentane, and the products eluted immediately with this solvent. Solvent removal gave 336 mg (65% yield) of a mixture of **67** and **68** in a 76:24 ratio as a yellow oil. The relatively unstable chlorides were stored in a pentane solution at −20 °C. Chlorides **67** and **68** gave no parent peak during the attempted HRMS analysis. ^{1}H NMR (600 MHz, $CDCl_3$): δ 7.87−7.77 (m, 2 H), 7.53−7.46 (m, 3 H), 2.98−2.87 (m, 2 H), 2.76−2.6 (m, 2 H), 2.14 (t of t, J = 10.4, 9.7 Hz, 0.26 H), 1.85 (t of t, J = 11.0, 9.2 Hz, 0.74 H), 0.07 (s, 6.66 H), 0.02 (s, 2.34 H). ^{13}C{^{1}H} NMR of **67** (150 MHz, $CDCl_3$): δ 151.2, 131.3, 129.10, 122.98, 91.3, 39.2, 15.3, −3.5. ^{13}C{^{1}H} NMR of **68** (150 MHz, $CDCl_3$): δ 151.1, 131.5, 129.09, 123.00, 92.6, 37.9, 13.4, −3.4.

Reaction of Chlorides 67 and 68 in CH_3CO_2H. Chlorides **67** and **68** (53 mg; 0.199 mmol) in 5 mL of CH_3CO_2H containing 24 mg of 2,6-lutidine (0.224 mmol) were kept at 30−35 °C for 22.5 h. The mixture was taken up into 10 mL of ether and 15 mL of pentane. The solution was washed with three portions of water and then a dilute $NaHCO_3$ solution. After drying with Na_2SO_4 and $MgSO_4$, the solution was filtered, and the solvents were removed using a rotary evaporator. The residue was filtered through 300 mg of silica gel using 3% ether in pentane. Solvent removal gave 53 mg (92% yield) of a mixture of **71a** and **72a** as a yellow oil. The **71a**:**72a** ratio was determined to be 69:31 by the integration of the acetoxy signals at δ 2.16 and 2.21. ^{1}H NMR of **71a** (600 MHz, $CDCl_3$): δ 7.75 (m, 2 H), 7.48−7.41 (m, 3 H), 2.70 (m, 2 H), 2.41 (m, 2 H), 2.16 (s, 3 H), 1.77 (m, 1 H), 0.048 (s, 9 H). ^{13}C{^{1}H} NMR of **71a** (150 MHz, $CDCl_3$): δ 169.4, 151.5, 130.8, 128.95, 122.7, 99.4, 34.6, 21.3, 12.9, −3.6. ^{1}H NMR of **72a** (600 MHz, $CDCl_3$): δ 7.72 (m, 2 H), 7.48−7.41 (m, 3 H), 2.67−2.62 (m, 4 H), 2.21 (s, 3 H), 1.78 (m, 1 H), 0.05 (s, 9 H). ^{13}C{^{1}H} NMR of **72a** (150 MHz, $CDCl_3$): δ 169.7, 151.3, 130.9, 128.93, 122.8, 100.9, 33.5, 21.6, 11.9, −3.1. HRMS (ESI): m/z (M + Na)$^+$ calculated for $C_{15}H_{22}N_2NaO_2Si$ 313.1343, found 313.1331.

Reaction of Chlorides 67 and 68 in CH_3OH. A solution of 17.8 mg of chlorides **67** and **68** (0.067 mmol) in 3 mL of CH_3OH was kept at room temperature for 145 min. A $NaOCH_3$ solution (0.16 mL of 0.510 M in methanol, 0.082 mmol) was added, and solvent was then removed using a rotary evaporator. Pentane (3 mL) was then added, and the mixture was washed with three portions of water. After drying over a mixture of Na_2SO_4 and $MgSO_4$, solvents were removed using a rotary evaporator. The crude products were filtered through 0.5 g of silica gel using 2% ether in pentane. Solvent removal using a rotary evaporator gave 14.1 mg (80% yield) of a mixture of methyl ethers **71b** and **72b** as a yellow oil. The **71b**:**72b** ratio was determined to be 73:27 by the integration of the methoxy signals at δ 3.35 and 3.45. ^{1}H NMR of **71b** (600 MHz, $CDCl_3$): δ 7.80 (m, 2 H), 7.50−7.43 (m, 3 H), 3.35 (s, 3 H), 2.43 (m, 2 H), 2.15 (m, 2 H), 1.35 (quintet, 1 H), 0.03 (s, 9 H). ^{13}C{^{1}H} NMR of **71b** (150 MHz, $CDCl_3$): δ 151.8, 130.8, 129.005, 122.6, 99.4, 50.8, 32.1, 9.8, −3.5. ^{1}H NMR of **72b** (600 MHz, $CDCl_3$): δ 7.76 (m, 2 H), 7.50−7.43 (m, 3 H), 2.38 (m, 2 H), 2.32 (m, 2 H), 1.65 (quintet, 1 H), −0.01 (s, 9 H). ^{13}C{^{1}H} NMR of **72b** (150 MHz, $CDCl_3$): δ 151.6, 130.9, 129.012, 122.6, 100.8, 51.1, 31.5, 10.9, −3.3. HRMS (ESI): m/z (M + H)$^+$ calculated for $C_{14}H_{23}N_2OSi$ 263.1574, found 263.1588.

Solvolytic Reactions. Details of the reactions of various substrates in various solvents are given in the Supporting Information.

Kinetics Studies. All the details, as well as the pertinent first-order plots, are given in the Supporting Information.

Computational Studies. Molecular orbital calculations were performed using the Gaussian 16 series of programs.[17] Structures were characterized as energy minima via frequency calculations that showed no negative frequencies. All transition states showed one imaginary frequency. Values of E represent electronic energies and do not include ZPVE (which are given in the Supporting Information).

■ ASSOCIATED CONTENT

Supporting Information

The Supporting Information is available free of charge at https://pubs.acs.org/doi/10.1021/acs.joc.1c00140.

Complete reference ref 17, details of the reactions of substrates in various solvents, data used for the determination of rate constants, ^{1}H and ^{13}C NMR spectra of new compounds, and computational details (PDF)

FAIR data, including the primary NMR FID files, for compounds **20**, **25**, **26**, **46**−**48**, **55**−**57**, **67**/**68**, **71a**/**72a**, and **71b**/**72b** (ZIP)

■ AUTHOR INFORMATION

Corresponding Author

Xavier Creary − *Department of Chemistry and Biochemistry, University of Notre Dame, Notre Dame, Indiana 46556, United States;* orcid.org/0000-0002-1274-5769; Email: creary.1@nd.edu

Complete contact information is available at: https://pubs.acs.org/10.1021/acs.joc.1c00140

Notes

The author declares no competing financial interest.

■ REFERENCES

(1) (a) *The Chemistry of the Hydrazo, Azo and Azoxy Groups, Vol. 1*; Patai, S., Ed.; Patai's Chemistry of Functional Groups; John Wiley & Sons: New York, NY, 1975. (b) *The Chemistry of the Hydrazo, Azo and Azoxy Groups, Vol. 2*; Patai, S., Ed.; Patai's Chemistry of Functional Groups; John Wiley & Sons: New York, NY, 1997.

(2) (a) Bafana, A.; Devi, S. S.; Chakrabarti, T. Azo Dyes: Past, Present and the Future. *Environ. Rev.* **2011**, *19*, 350−371. (b) Chung, K.-T. Azo Dyes and Human Health: A Review. *J. Environ. Sci. Health, Part C* **2016**, *34*, 233−261. (c) Benkhaya, S.; M'rabet, S.; Harfi, A. E. Classifications, Properties, Recent Synthesis and Applications of Azo Dyes. *Heliyon* **2020**, *6*, e03271.

(3) Ali, Y.; Hamid, S. A.; Rashid, U. Biomedical Applications of Aromatic Azo Compounds. *Mini-Rev. Med. Chem.* **2018**, *18*, 1548−1558.

(4) (a) Overberger, C. G.; O'Shaughnessy, M. T.; Shalit, H. The Preparation of Some Aliphatic Azo Nitriles and their Decomposition in Solution. *J. Am. Chem. Soc.* **1949**, *71*, 2661−2666. (b) Onishi, Y.; Kodaira, K.; Ito, K. Some Unsymmetrical Azo Compounds as Initiators in Radical Polymerization. *Polymer* **1982**, *23*, 630−631. (c) Braun, D. Origins and Development of Initiation of Free Radical Polymerization Processes. *Int. J. Polym. Sci.* **2009**, *2009*, 1−10. (d) Nesvadba, P. Radical Polymerization in Industry. *Encyclopedia of Radicals in Chemistry, Biology and Materials* **2012**, DOI: 10.1002/9781119953678.rad080.

(5) For a summary and leading references, see: Vetráková, K.; Ladányi, V.; Anshori, J. A.; Dvořák, P.; Wirz, J.; Heger, D. The Absorption Spectrum of *cis*-Azobenzene. *Photochem. Photobiol. Sci.* **2017**, *16*, 1749−1756.

(6) Creary, X.; Engel, P. S.; Kavaluskas, N.; Pan, L.; Wolf, A. Methylenecyclopropane Rearrangement as a Probe for Free Radical Substituent Effects. σ • Values for Potent Radical Stabilizing Nitrogen-Containing Substituents. *J. Org. Chem.* **1999**, *64*, 5634−5643.
(7) Creary, X. Electronegatively Substituted Carbocations. *Chem. Rev.* **1991**, *91*, 1625−1678.
(8) (a) Gassman, P. G.; Tidwell, T. T. Electron-deficient Carbocations. *Acc. Chem. Res.* **1983**, *16*, 279−285. (b) Tidwell, T. T. Destabilized Carbocations. *Angew. Chem., Int. Ed. Engl.* **1984**, *23*, 20−32.
(9) (a) Gassman, P. G.; Talley, J. J. The α-Cyano Group as a Substituent in Solvolysis Reactions. An Evaluation of Inductive Destabilization vs. Mesomeric Stabilization of Cations by the Cyano Moiety. *J. Am. Chem. Soc.* **1980**, *102*, 1214−1216. (b) Dixon, D. A.; Charlier, P. A.; Gassman, P. G. Mesomeric Stabilization of Carbonium Ions by α-Cyano Groups. A Theoretical Evaluation of Inductive vs. Resonance Effects of the Cyano Moiety. *J. Am. Chem. Soc.* **1980**, *102*, 3957−3959. (c) Gassman, P. G.; Guggenheim, T. L. Influence of an α-Cyano Function on Charge Delocalization in the Benzyl Cation. Relationship between Inductive Destabilization and Conjugative Stabilization by the Cyano Group. *J. Org. Chem.* **1982**, *47*, 3023−3026.
(10) Creary, X.; Geiger, C. C. Properties of α-Keto Cations. Facile Generation under Solvolytic Conditions. *J. Am. Chem. Soc.* **1982**, *104*, 4151−4162.
(11) Creary, X.; Hatoum, H. N.; Barton, A.; Aldridge, T. E. Solvolytic Elimination Reactions of Tertiary α-CSNMe$_2$ Cations. *J. Org. Chem.* **1992**, *57*, 1887−1897.
(12) Creary, X.; Wang, Y.-X.; Jiang, Z. α-Imino and α-Oximino Carbocations. A Comparison with α-Carbonyl and α-Thiocarbonyl Carbocations. *J. Am. Chem. Soc.* **1995**, *117*, 3044−3053.
(13) Takeuchi, K.; Yoshida, M.; Ohga, Y.; Tsugeno, A.; Kitagawa, T. Stability of 2-Oxo and 2-Methylene Bridgehead Carbocations in Solvolysis: Further Evidence for the Unimportance of π-Conjugative Stabilization in Tertiary α-Keto Cations. *J. Org. Chem.* **1990**, *55*, 6063−6065.
(14) Fisher, T. H.; Meierhoefer, A. W. On the nature of the phenylazo group. *Tetrahedron* **1975**, *31*, 2019−2021.
(15) Byrne, C. J.; Happer, D. A. R.; Hartshorn, M. P.; Powell, H. K. J. The electronic effect of the phenylazo and *t*-butylazo groups. *J. Chem. Soc., Perkin Trans. 2* **1987**, *2*, 1649−1653.
(16) (a) Hong, X.; Bercovici, D. A.; Yang, Z.; Al-Bataineh, N.; Srinivasan, R.; Dhakal, R. C.; Houk, K. N.; Brewer, M. Mechanism and Dynamics of Intramolecular C-H Insertion Reactions of 1-Aza-2-azoniaallene Salts. *J. Am. Chem. Soc.* **2015**, *137*, 9100−9107. (b) Bercovici, D. A.; Ogilvie, J. M.; Tsvetkov, N.; Brewer, M. Intramolecular Polar [$4^{\oplus}$+2] Cycloadditions of Aryl-1-aza-2-azoniaallene Salts: Unprecedented Reactivity Leading to Polycyclic Protonated Azomethine Imines. *Angew. Chem., Int. Ed.* **2013**, *52*, 13338−13341. (c) Bercovici, D. A.; Brewer, M. Stereospecific Intramolecular C-H Aminatiuon of 1-Aza-2-azoniaallene Salts. *J. Am. Chem. Soc.* **2012**, *134*, 9890−9893. (d) Wyman, J.; Javed, M. I.; Al-Bataineh, N.; Brewer, M. Synthetic Approaches to Bicyclic Diazenium Salts. *J. Org. Chem.* **2010**, *75*, 8078−8087. (e) Wirschun, W. G.; Al-Soud, Y. A.; Nusser, K. A.; Orama, O.; Maier, G. M.; Jochims, J. C. Cycloadditions of 1-Aza-2-azoniaallene Ions to Alkenes. *J. Chem. Soc., Perkin Trans.* **2000**, *1*, 4356−4365. (f) Wang, Q. R.; Amer, A.; Mohr, S.; Ertel, E.; Jochims, J. C. [3 + 2]-Cycloadditions of 1-Aza-2-azoniaallene Cations to Multiple Bonds. *Tetrahedron* **1993**, *49*, 9973−9986.
(17) Frisch, M. J.; Trucks, G. W.; Schlegel, H. B.; Scuseria, G. E.; Robb, M. A.; Cheeseman, J. R.; Scalmani, G.; Barone, V.; Petersson, G. A.; Nakatsuji, H., et al. *Gaussian 16*, rev. B.01; Gaussian, Inc.: Wallingford, CT, 2016. See the Supporting Information for the entire reference.
(18) Tomasi, J.; Mennucci, B.; Cammi, R. Quantum Mechanical Continuum Solvation Models. *Chem. Rev.* **2005**, *105*, 2999−3093.
(19) Dokić, J.; Gothe, M.; Wirth, J.; Peters, M. V.; Schwarz, J.; Hecht, S.; Saalfrank, P. Quantum Chemical Investigation of Thermal *Cis*-to-*Trans* Isomerization of Azobenzene Derivatives: Substituent Effects, Solvent Effects, and Comparison to Experimental Data. *J. Phys. Chem. A* **2009**, *113*, 6763−6773.
(20) (a) Smith, S.; Bou-Abdallah, F. The Kinetics of the *Cis*-to-*Trans* Thermal Isomerization of 4-Anilino-4'-Nitroazobenzene are Highly Influenced by Solvent Polarity. *J. Thermodyn. Catal.* **2017**, *8*, 181. (b) Angelini, G.; Canilho, N.; Emo, M.; Kingsley, M.; Gasbarri, C. Role of Solvent and Effect of Substituent on Azobenzene Isomerization by Using Room-Temperature Ionic Liquids as Reaction Media. *J. Org. Chem.* **2015**, *80*, 7430−7434. (c) Joshi, N. K.; Fuyuki, M.; Wada, A. Polarity Controlled Reaction Path and Kinetics of Thermal *cis*-to-*trans* Isomerization of 4-Aminoazobenzene. *J. Phys. Chem. B* **2014**, *118*, 1891−1899. (d) Asano, T.; Okada, T.; Shinkai, S.; Shigematsu, K.; Kusano, Y.; Manabe, O. Temperature and Pressure Dependences of Thermal *Cis*-to-*Trans* Isomerization of Azobenzenes Which Evidence an Inversion Mechanism. *J. Am. Chem. Soc.* **1981**, *103*, 5161−5165. (e) Asano, T.; Yano, T.; Okada, T. Mechanistic Study of Thermal *Z-E* Isomerization of Azobenzenes by High Pressure Kinetics. *J. Am. Chem. Soc.* **1982**, *104*, 4900−4904.
(21) Creary, X. Reaction of Organometallic Reagents with Ethyl Trifluoroacetate and Diethyl Oxalate. Formation of Trifluoromethyl Ketones and α-Keto Esters via Stable Tetrahedral Adducts. *J. Org. Chem.* **1987**, *52*, 5026.
(22) (a) Richard, J. P.; Jencks, W. P. A Simple Relationship between Carbocation Lifetime and Reactivity-Selectivity Relationships for the Solvolysis of Ring-Substituted 1-Phenylethyl Derivatives. *J. Am. Chem. Soc.* **1982**, *104*, 4689−4691. (b) Richard, J. P.; Amyes, T. L.; Jagannadham, V.; Lee, Y.-G.; Rice, D. J. Spontaneous Cleavage of gem-Diazides: A Comparison of the Effects of α-Azido and Other Electron-Donating Groups on the Kinetic and Thermodynamic Stability of Benzyl and Alkyl Carbocations in Aqueous Solution. *J. Am. Chem. Soc.* **1995**, *117*, 5198−5205.
(23) (a) McClelland, R. A.; Banait, N.; Steenken, S. Electrophilic Reactivity of the Triphenylmethyl Carbocation in Aqueous Solution. *J. Am. Chem. Soc.* **1986**, *108*, 7023−7027. (b) Richard, J. P.; Rothenberg, M. E.; Jencks, W. P. Formation and Stability of Ring-Substituted 1-Phenylethyl Carbocations. *J. Am. Chem. Soc.* **1984**, *106*, 1361−1372.
(24) Hong, X.; Liang, Y.; Brewer, M.; Houk, K. N. How Tethers Control the Chemo- and Regioselectivities of Intramolecular Cycloadditions between Aryl-1-aza-2-azoniaallenes and Alkenes. *Org. Lett.* **2014**, *16*, 4260−4263.
(25) Creary, X.; Heffron, A.; Going, G.; Prado, M. γ-Trimethylsilylcyclobutyl Carbocation Stabilization. *J. Org. Chem.* **2015**, *80*, 1781−1788.
(26) (a) Mercadante, M. A.; Kelly, C. B.; Hamlin, T. A.; Chiaie, K. R. D; Drago, M. D.; Duffy, K. K.; Dumas, M. T.; Fager, D. C.; Glod, B. L. C.; Hansen, K. E.; Hill, C. R.; Leising, R. M.; Lynes, C. L.; MacInnis, A. E.; McGohey, M. R.; Murray, S. A.; Piquette, M. C.; Roy, S. L.; Smith, R. M.; Sullivan, K. R.; Truong, B. H.; Vailonis, K. M.; Gorbatyuk, V.; Leadbeater, N. E.; Tilley, L. J. 1,3-γ-Silyl-Elimination in Electron-Deficient Cationic Systems. *Chem. Sci.* **2014**, *5*, 3983−3994. (b) Shiner, V. J., Jr.; Ensinger, M. W.; Huffman, J. C. γ-Silicon Stabilization of Carbonium Ions in Solvolysis. III: Solvolysis of 4-(Trimethylsilyl)-3-methyl-2-butyl *p*-Bromobenzenesulfonates. *J. Am. Chem. Soc.* **1989**, *111*, 7199−7205. (c) Adcock, W.; Clark, C. I.; Schiesser, C. H. Effects of Bridgehead Metalloidal Substituents (MMe$_3$, M = Si and Sn) on the Stability of the 1-Norbornyl Cation. *J. Am. Chem. Soc.* **1996**, *118*, 11541−11547. (d) Siehl, H.-U.; Fulj, M. Recent Advances in the Experimental and Computational Characterization of Carbocations: Silyl Effects in Bicyclobutonium Ions. *Pure Appl. Chem.* **1998**, *70*, 2015−2022. (e) Siehl, H.-U. The Conundrum of the $(C_4H_7)^+$ Cation: Bicyclobutonium and Related Carbocations. *Adv. Phys. Org. Chem.* **2018**, *52*, 1−47.
(27) (a) Stawski, P.; Sumser, M.; Trauner, D. A Photochromic Agonist of AMPA Receptors. *Angew. Chem., Int. Ed.* **2012**, *51*, 5748−5751. (b) Rao, J.; Hottinger, C.; Khan, A. Enzyme-Triggered Cascade Reactions and Assembly of Abiotic Block Copolymers into Micellar Nanostructures. *J. Am. Chem. Soc.* **2014**, *136*, 5872−5875. (c) Agnetta, L.; Bermudez, M.; Riefolo, F.; Matera, C.; Claro, R.; Messerer, R.; Littmann, T.; Wolber, G.; Holzgrabe, U.; Decker, M. Fluorination of

https://dx.doi.org/10.1021/acs.joc.1c00140
J. Org. Chem. XXXX, XXX, XXX−XXX

Photoswitchable Muscarinic Agonists Tunes Receptor Pharmacology and Photochromic Properties. *J. Med. Chem.* **2019**, *62*, 3009−3020.
(28) Yu, B.-C.; Shirai, Y.; Tour, J. M. Synthesis of New Functionalized Azobenzenes for Potential Molecular Electronic Devices. *Tetrahedron* **2006**, *62*, 10303−10310.
(29) (a) Keyhani, S.; Goldau, T.; Blümler, A.; Heckel, A.; Schwalbe, H. Chemo-Enzymatic Synthesis of Position-Specifically Modified RNA for Biophysical Studies including Light Control and NMR Spectroscopy. *Angew. Chem., Int. Ed.* **2018**, *57*, 12017−12021. (b) Unno, M.; Kakiage, K.; Yamamura, M.; Kogure, T.; Kyomen, T.; Hanaya, M. Silanol Dyes for Solar Cells; Higher Efficiency and Significant Durability. *Appl. Organomet. Chem.* **2010**, *24*, 247−250.
(30) (a) Rostovtsev, V. V.; Green, L. G.; Fokin, V. V.; Sharpless, K. B. A Stepwise Huisgen Cycloaddition Process: Copper(I)-Catalyzed Regioselective "Ligation" of Azides and Terminal Alkynes. *Angew. Chem., Int. Ed.* **2002**, *41*, 2596−2599. (b) Tornøe, C. W.; Christensen, C.; Meldal, M. Peptidotriazoles on Solid Phase: [1,2,3]-Triazoles by Regiospecific Copper(I)-Catalyzed 1,3-Dipolar Cycloadditions of Terminal Alkynes to Azides. *J. Org. Chem.* **2002**, *67*, 3057−3064.

https://dx.doi.org/10.1021/acs.joc.1c00140
J. Org. Chem. XXXX, XXX, XXX−XXX